RESEARCH BRIEF

Acquired Resistance to the TRK Inhibitor Entrectinib in Colorectal Cancer

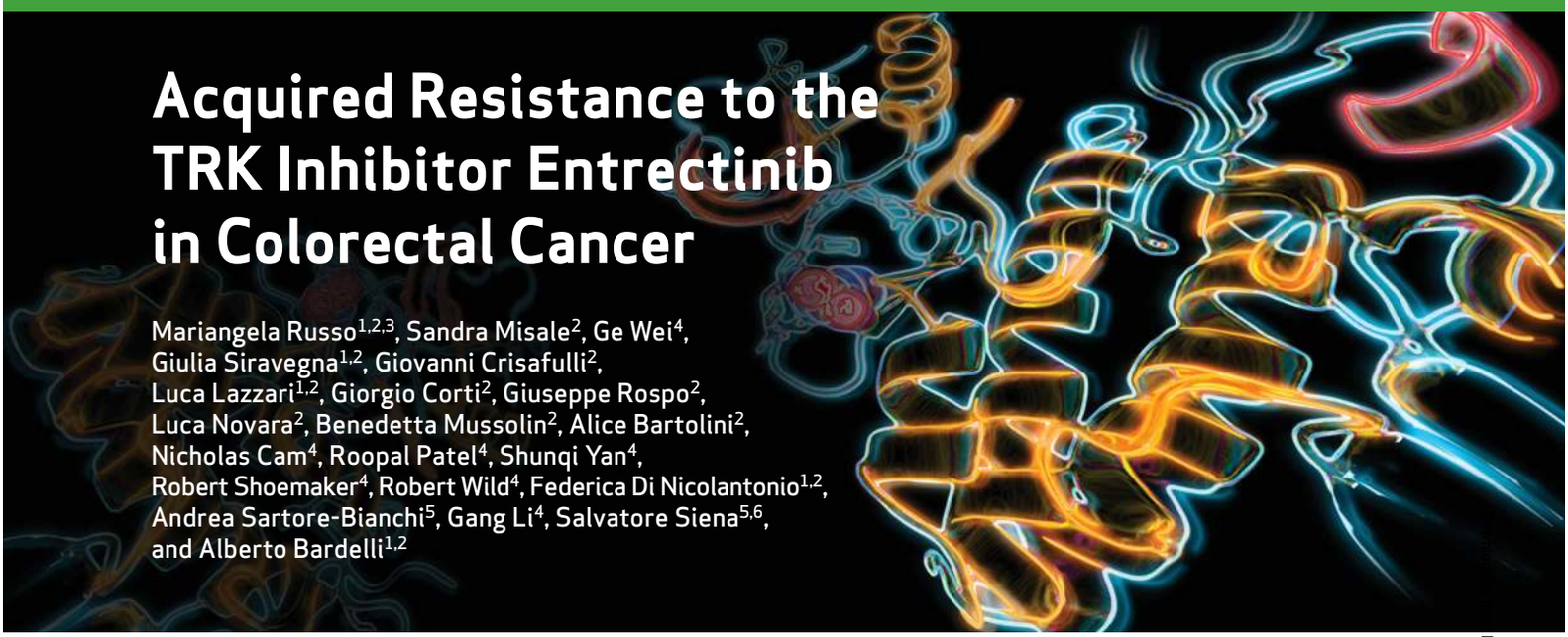

Mariangela Russo[1,2,3], Sandra Misale[2], Ge Wei[4], Giulia Siravegna[1,2], Giovanni Crisafulli[2], Luca Lazzari[1,2], Giorgio Corti[2], Giuseppe Rospo[2], Luca Novara[2], Benedetta Mussolin[2], Alice Bartolini[2], Nicholas Cam[4], Roopal Patel[4], Shunqi Yan[4], Robert Shoemaker[4], Robert Wild[4], Federica Di Nicolantonio[1,2], Andrea Sartore-Bianchi[5], Gang Li[4], Salvatore Siena[5,6], and Alberto Bardelli[1,2]

ABSTRACT

Entrectinib is a first-in-class pan-TRK kinase inhibitor currently undergoing clinical testing in colorectal cancer and other tumor types. A patient with metastatic colorectal cancer harboring an *LMNA–NTRK1* rearrangement displayed a remarkable response to treatment with entrectinib, which was followed by the emergence of resistance. To characterize the molecular bases of the patient's relapse, circulating tumor DNA (ctDNA) was collected longitudinally during treatment, and a tissue biopsy, obtained before entrectinib treatment, was transplanted in mice (xenopatient), which then received the same entrectinib regimen until resistance developed. Genetic profiling of ctDNA and xenopatient samples showed acquisition of two point mutations in the catalytic domain of *NTRK1*, p.G595R and p.G667C. Biochemical and pharmacologic analysis in multiple preclinical models confirmed that either mutation renders the TRKA kinase insensitive to entrectinib. These findings can be immediately exploited to design next-generation TRKA inhibitors.

SIGNIFICANCE: We provide proof of principle that analyses of xenopatients (avatar) and liquid biopsies allow the identification of drug resistance mechanisms in parallel with clinical treatment of an individual patient. We describe for the first time that p.G595R and p.G667C TRKA mutations drive acquired resistance to entrectinib in colorectal cancers carrying *NTRK1* rearrangements. *Cancer Discov; 6(1); 36–44. ©2015 AACR.*

See related commentary by Okimoto and Bivona, p. 14.

INTRODUCTION

TRK receptors are a family of tyrosine kinases that comprises three members: TRKA, TRKB, and TRKC, encoded by the neurotrophic tyrosine kinase receptor, type 1 (*NTRK1*), *NTRK2*, and *NTRK3* genes, respectively. Genomic rearrangement is the most common mechanism of oncogenic activation for this family of receptors, resulting in sustained cancer cell proliferation through activation of MAPK and AKT downstream pathways (1). Rearrangements of the *NTRK1*, *NTRK2*, and *NTRK3* genes occur across different tumors, including colorectal cancers (2).

[1]Department of Oncology, University of Torino, Torino, Italy. [2]Candiolo Cancer Institute, FPO, IRCCS, Torino, Italy. [3]FIRC Institute of Molecular Oncology (IFOM), Milano, Italy. [4]Ignyta, Inc., San Diego, California. [5]Department of Hematology and Oncology, Niguarda Cancer Center, Ospedale Niguarda Ca' Granda, Milan, Italy. [6]Università degli Studi di Milano, Milan, Italy.

Note: Supplementary data for this article are available at Cancer Discovery Online (http://cancerdiscovery.aacrjournals.org/).

M. Russo, S. Misale, and G. Wei contributed equally to this article.

A. Bardelli and S. Siena share senior authorship of this article.

Corresponding Author: Alberto Bardelli, Department of Oncology, University of Torino, Candiolo Cancer Institute, FPO, IRCCS, strada provinciale 142, km 3.95, Candiolo 10060, Torino, Italy. Phone: 39-011-9933235; Fax: 39-011-9933225; E-mail: alberto.bardelli@unito.it

doi: 10.1158/2159-8290.CD-15-0940

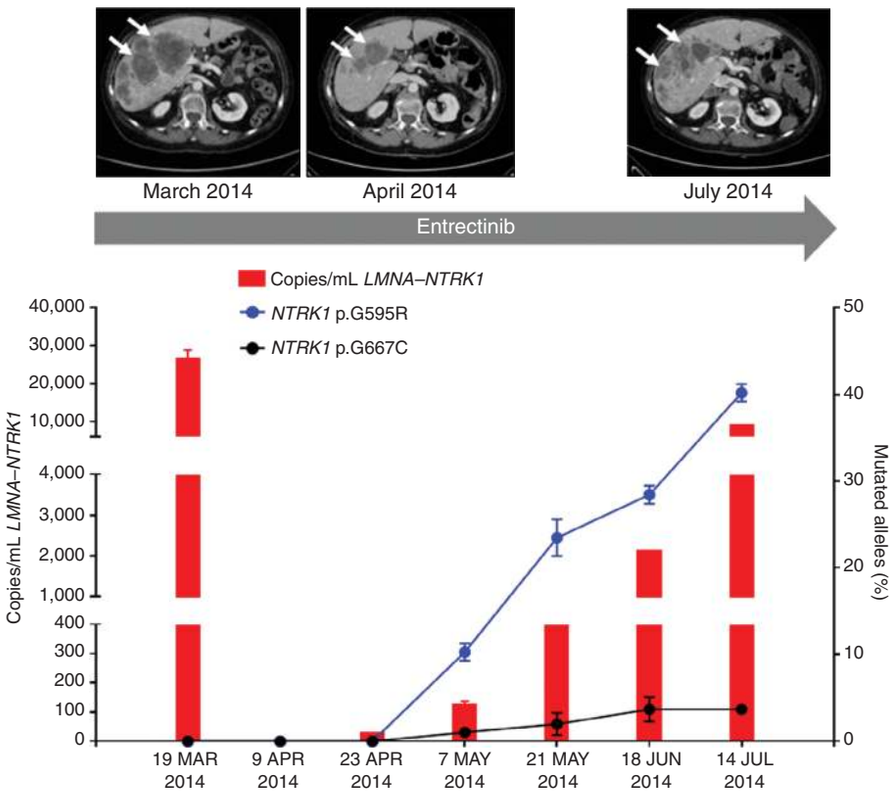

Figure 1. Tracking resistance to TRKA inhibition in ctDNA of a patient with colorectal cancer. Top, CT scans of a patient with metastatic colorectal cancer harboring an *LMNA–NTRK1* rearrangement were recorded at baseline (March 2014), at the time of partial response to the pan-TRK inhibitor entrectinib (April 2014), and upon disease progression (July 2014). Bottom, longitudinal analysis of plasma ctDNA collected at different time points throughout the treatment. Red bars, absolute *LMNA–NTRK1* copies in 1 mL of plasma; blue and black lines, *NTRK1* p.G595R- and p.G667C-mutated alleles (%), respectively. Average ± SD of 3 independent experiments is reported.

Entrectinib (RXDX-101, previously known as NMS-E628) is a potent pan-TRK, ALK, and ROS1 inhibitor, currently undergoing phase I clinical trials (3). During treatment with entrectinib, a patient with metastatic colorectal cancer harboring an *LMNA–NTRK1* rearrangement showed a remarkable response. We reasoned that, as it has been shown for most targeted agents, response to entrectinib might be limited in time due to the emergence of acquired resistance. Nothing is presently known about the mechanisms of resistance to entrectinib and consequently further lines of treatment are not available. We postulated that it might be possible to identify the resistance mechanism(s) while the patient was being treated by analyzing circulating tumor DNA (ctDNA) and developing a xenopatient (avatar).

RESULTS

Acquired Resistance to TRKA Inhibition in a Patient with Colorectal Cancer

A molecular screen identified a genetic rearrangement involving exon 10 of *NTRK1* and exon 11 of the *LMNA* genes (4) in a patient with metastatic colorectal cancer whose disease was intrinsically resistant to first-line FOLFOX, second-line FOLFIRI/cetuximab, and third-line irinotecan. We and others have previously reported that colorectal cancer cell models harboring *NTRK1* translocations are sensitive to *NTRK1* silencing and to TRKA (protein encoded by the *NTRK1* gene) kinase inhibition (5–7). Based on this, the patient was enrolled in the phase I ALKA clinical trial (EudraCT Number 2012-000148-88) of the pan-TRK kinase inhibitor entrectinib, a first-in-class drug currently undergoing clinical testing (3). The patient received entrectinib on an intermittent dosing schedule of 4 days on/3 days off for 3 weeks followed by a week break in every 28-day cycle (4). Treatment was remarkably effective and well tolerated, leading to a partial response (PR) with 30% tumor shrinkage of multiple liver metastases that was demonstrated by an early CT scan assessment performed after 30 days of treatment. The clinical response lasted 4 months, followed by the emergence of drug resistance as evaluated by Response Evaluation Criteria in Solid Tumor (RECIST) progression (Fig. 1, top).

Emergence of *NTRK1* Mutations in ctDNA during Entrectinib Treatment

To unveil the molecular basis of acquired resistance to TRKA inhibition, we analyzed ctDNA, a form of liquid biopsy (8) we previously optimized to detect and monitor drug resistance in patients treated with targeted agents (9, 10).

ctDNA extracted from plasma samples collected before treatment initiation and at clinical relapse was subjected to molecular profiling using the IRCC-TARGET panel, a next-generation sequencing (NGS) platform based on 226 cancer-related genes which we optimized to detect with high sensitivity mutations in ctDNA (10). Profiling of ctDNA at entrectinib resistance revealed two novel *NTRK1* genetic alterations in the kinase domain of the protein, p.G595R and p.G667C, which were not detected in ctDNA obtained before initiation of therapy (Supplementary Tables S1 and S2). To monitor the *NTRK1*-mutated alleles in the patient's plasma collected throughout the treatment, droplet digital PCR (ddPCR; refs. 11, 12) assays were designed for both mutations. As a means of tracking the overall disease, a ddPCR assay was also optimized to detect the *LMNA–NTRK1* rearrangement in ctDNA.

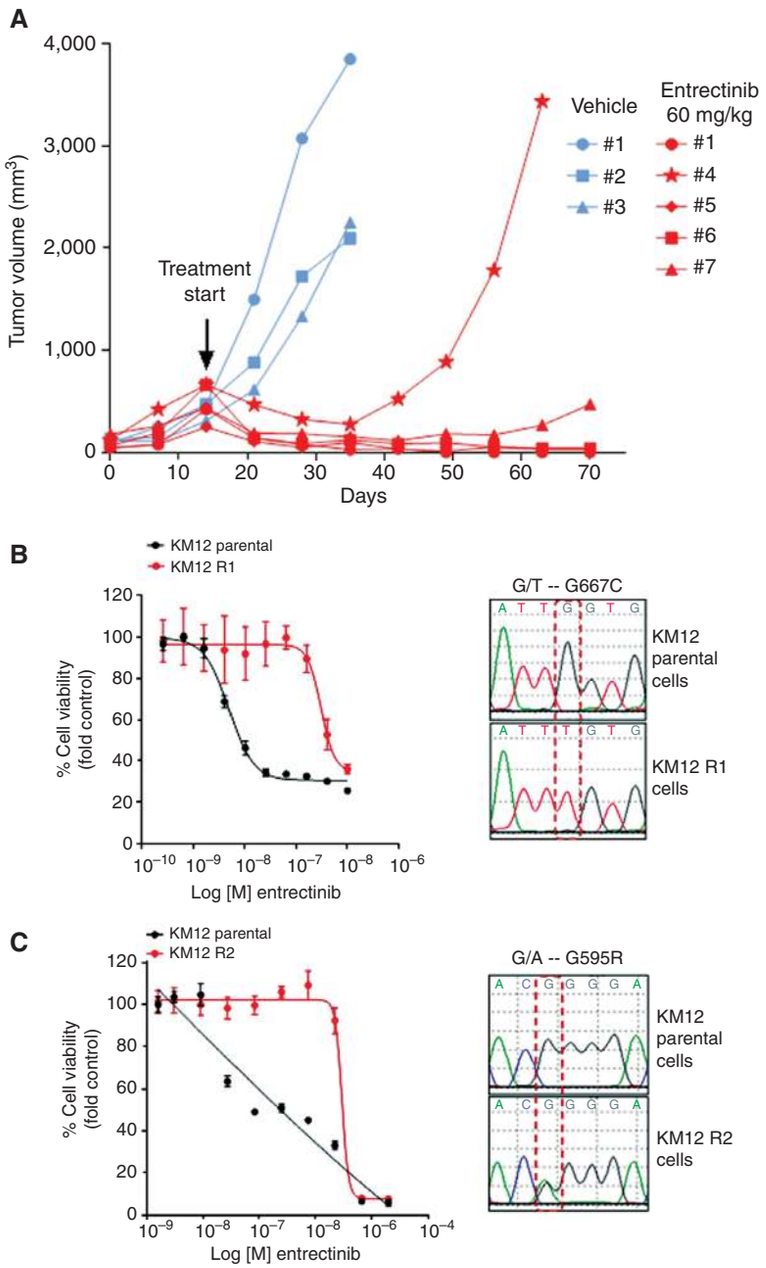

Figure 2. Resistance to entrectinib in xenopatient and colorectal cancer cell models carrying *NTRK1* translocations. **A,** bioptic specimen obtained from a thin needle biopsy of a patient with metastatic colorectal cancer harboring an *LMNA–NTRK1* rearrangement was first implanted subcutaneously in an immunocompromised mouse and then expanded in multiple mice upon successful engraftment. Mice were treated with dosage levels and schedules (60 mg/kg, 4 days/week) that yielded clinically relevant exposure achievable in patients. After 3 weeks of treatment, a mouse (#4) in the treated arm relapsed. Blue and red lines, vehicle- and entrectinib-treated mice, respectively. **B,** proliferation assay of KM12 (carrying a *TPM3–NTRK1* rearrangement) R1 cells made resistant to a low dose of entrectinib (300 nmol/L). Cell viability was assessed by measuring ATP content after 5 days of treatment. Sanger sequencing electropherogram of KM12 R1 shows *NTRK1* p.G667C mutation. **C,** proliferation assay of KM12 (carrying an *TPM3–NTRK1* rearrangement) R2 cells made resistant to a high dose of entrectinib (2 μmol/L). Cell viability was assessed by measuring ATP content after 5 days of treatment. Sanger sequencing electropherogram of KM12 R2 shows an *NTRK1* p.G595R mutation.

Longitudinal analysis of plasma revealed that the p.G595R- and p.G667C-mutated alleles were initially absent in ctDNA but emerged in the circulation as early as 4 weeks upon initiation of treatment with entrectinib (Fig. 1). *NTRK1* mutation frequencies continued to increase in ctDNA and peaked when clinical progression was radiologically confirmed (16 weeks after initiation of treatment). The profile of the *LMNA–NTRK1* rearrangement in ctDNA paralleled tumor response and resistance to entrectinib (Fig. 1 and Supplementary Table S3).

Secondary Resistance to Entrectinib in a Colorectal Cancer Xenopatient

To functionally evaluate the mechanistic basis of resistance to entrectinib, a biopsy specimen gathered before initiation of treatment was transplanted subcutaneously in an immunocompromised mouse (xenopatient; see Supplementary Methods). Upon successful engraftment, the tumor was expanded in multiple mice, which were treated with dosage levels and schedules that matched clinically relevant exposure achievable in patients. Entrectinib induced remarkable tumor shrinkage in the xenopatient, whereas vehicle-treated tumors grew exponentially (Fig. 2A). After 3 weeks of drug dosing, one of the tumors treated with entrectinib rapidly developed resistance to TRKA inhibition (Fig. 2A). NGS-based molecular profiling of this resistant sample using the IRCC-TARGET panel unveiled the *LMNA–NTRK1* rearrangement peculiar to the patient and the *NTRK1* p.G595R mutation, which could not be detected in the untreated tumor

(Supplementary Fig. S1A and S1B; Supplementary Tables S1 and S2).

Secondary Resistance to Entrectinib in Cells Carrying *NTRK1* Rearrangements

To assess whether the mechanism of resistance was patient specific or contingent on the peculiar *NTRK1* rearrangements, independent models of acquired resistance to entrectinib were established. The KM12 colorectal cancer cell line harbors a distinct genetic rearrangement involving exon 10 of the *NTRK1* and exon 7 of *TPM3* genes (5, 7) and is also highly sensitive to entrectinib (Fig. 2B and C). Independent batches of parental (sensitive) KM12 cells were exposed to either acute constant dose (R2) or escalating doses (R1) of entrectinib until resistant derivatives emerged (Fig. 2B and C; see Supplementary Methods). Molecular profiling of the cells that became resistant to lower concentrations of entrectinib (30–100 nmol/L; named KM12 R1) revealed the missense mutation p.G667C in the kinase domain of *NTRK1*, previously identified also in the plasma of the patient (Fig. 2B). When cells were made resistant to higher doses (1–2 μmol/L) of the drug (named KM12 R2), the *NTRK1* p.G595R alteration was detected (Fig. 2C). The experiment was repeated multiple times, and the two mutations were never concomitantly detected in the same resistant populations, indicating they occurred in independent cells.

To further evaluate the mechanisms of entrectinib resistance, we engineered Ba/F3 cells to express ETV6–TRKA. In this model system, the ETV6 domain mimics the dimerization effect of TRK fusion partners that occur in human tumors. Ba/F3 cells engineered to express ETV6–TRKA became exquisitely sensitive to entrectinib (Supplementary Fig. S2). ETV6–TRKA Ba/F3 cells were then exposed to entrectinib treatment until resistant derivatives emerged and were analyzed as described above. Remarkably, upon development of resistance, Ba/F3 also acquired the p.G595R mutation in the kinase domain of TRKA when a high dose of entrectinib was applied, whereas the p.G667C allele emerged in the presence of a lower dose of the drug (Supplementary Fig. S2). Analogous to what we observed in KM12, the two mutations were found in independent pools of Ba/F3 cells, indicating they do not co-occur in the same cells.

NTRK1 p.G595R and p.G667C Mutations Drive Resistance to TRK Inhibitors

We then examined the impact of the p.G595R and p.G667C variants on the three-dimensional (3-D) structure of the TRKA catalytic domain (see Supplementary Methods). The binding model of entrectinib with wild-type (WT) TRKA highlighted that entrectinib makes extensive hydrogen bonding as well as hydrophobic interactions with the protein in the ATP pocket where p.G595 and p.G667 residues are located (Fig. 3A). The p.G595R and p.G667C mutations create steric hindrance that either abrogates binding (p.G595R) or reduces the binding affinity (p.G667C) of entrectinib to the TRKA catalytic pocket (Fig. 3B and C, respectively).

We next assessed whether and to what extent mutations in the kinase domain of *NTRK1* drive resistance to TRKA inhibition. We engineered Ba/F3 cells expressing wild-type, p.G595R, or p.G667C TPM3–TRKA fusion proteins. We then measured the sensitivity of *NTRK1*-mutated cells to TRK inhibitors currently in clinical development. LOXO-101 is a TRK inhibitor in a phase I trial for patients with advanced solid tumors with *NTRK* alterations (NCT02122913); TSR-011 is presently undergoing a phase I trial for patients with advanced solid tumors or lymphomas with *NTRK* alterations (NCT02048488).

As shown in Supplementary Fig. S3, Ba/F3 cells harboring the *NTRK1* translocation become highly sensitive to TRK inhibitors (Supplementary Fig. S3A and S3B; Supplementary Table S4). On the contrary, *NTRK1* p.G595R or p.G667C mutations are resistant to entrectinib, LOXO-101, and TSR-011 (Supplementary Fig. S3C and S3D, respectively). Of potential clinical relevance, and in line with previous results, *NTRK1* p.G595R appears to be more potent in conferring resistance than p.G667C.

These results are indeed consistent with the observation that entrectinib and LOXO-101 retain a partial effect on p.G667C (IC_{50} = 61 and 524 nmol/L, respectively) but are totally ineffective on p.G595R (IC_{50} > 1000 nmol/L) in Ba/F3–engineered cells (Supplementary Table S4).

Alignment of the TRKA kinase domain with clinically targeted tyrosine kinases, such as ALK, ROS, EGFR, MET, and KIT, showed that the glycine residues at positions 595 and 667 lie in a conserved region (Supplementary Fig. S4A and S4B, respectively), and are analogous to residues previously found to be associated with secondary resistance to other kinase inhibitors, such as erlotinib, crizotinib, and imatinib (Fig. 3D and E, respectively).

Biochemical Characterization of *NTRK1* p.G595C and p.G667C in Xenopatient-Derived Cells

To mechanistically study the impact of *NTRK1* resistant alleles, we established two cell lines, one from the xenopatient treated with vehicle, and the other from the xenopatient who became resistant to entrectinib (Fig. 4A). Both cell lines displayed the *LMNA–NTRK1* translocation found in the patient tumor (Fig. 4B), but only cells derived from the xenotumor that had become resistant to entrectinib carried the p.G595R allele (Fig. 4C). Both cell lines displayed a pharmacologic response to entrectinib analogous to that observed in the corresponding xenopatients (Fig. 4D). Biochemical characterization confirmed that *NTRK1* secondary mutations render the corresponding proteins insensitive (or only marginally sensitive) to entrectinib and capable of activating downstream signaling in the presence of the drug (Fig. 4E and F). We next asked whether the tumor cell that had become resistant remained dependent on the expression of TRKA. Indeed, siRNA-mediated suppression of mutant *NTRK1* in resistant cells induced apoptosis, similar to the knockdown of WT *NTRK1* in sensitive cells (Fig. 4G).

DISCUSSION

A subset of colorectal cancers carries *NTRK1* translocations, which also occur in other tumor types, such as lung tumors and thyroid carcinomas (6, 13–15). The TRK inhibitor entrectinib induced a remarkable clinical response in a patient with a metastatic colorectal cancer carrying a *LMNA–NTRK1* translocation, whose disease was intrinsically refractory to

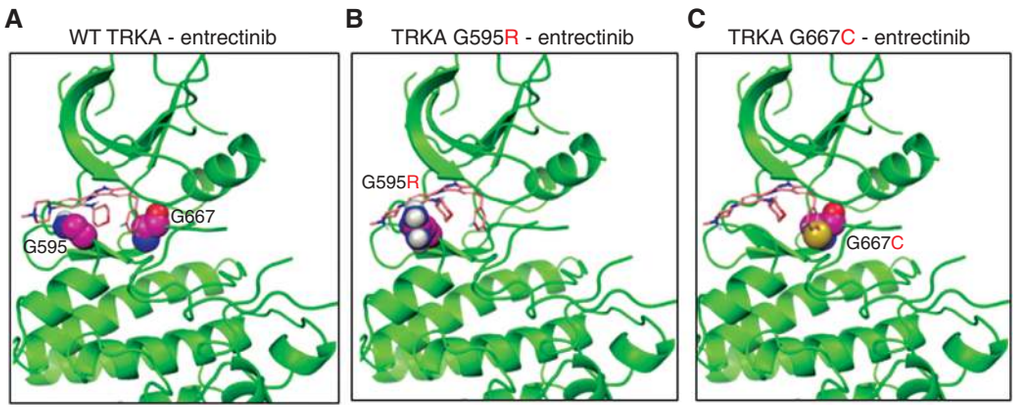

D

Gene	Codon	Mutation at resistance	Tissue of detection	Associated with resistance to
NTRK1	595	p.G595R	Colon	Entrectinib
ALK	1202	p.G1202R	Lung	Crizotinib/ceritinib
ROS1	2032	p.G2032R	Lung	Crizotinib
EGFR	796	p.G796A/R	Lung	Erlotinib/gefitinib

E

Gene	Codon	Mutation at resistance	Tissue of detection	Associated with resistance to
NTRK1	667	p.G667C	Colon	Entrectinib
ALK	1269	p.G1269A	Lung	Crizotinib
ROS1	2101	p.G2101A	Lung	Crizotinib
EGFR	854	p.T854A	Lung	Erlotinib/gefitinib
KIT	809	p.C809G	GIST	Imatinib

Figure 3. 3-D modeling and homology alignment of *NTRK1* p.G595 and p.G667 variants. **A–C,** modeled binding mode of entrectinib with wild-type TRKA (**A**), TRKA p.G595R (**B**), and TRKA p.G667C (**C**). G595R and G667C mutants create steric hindrance directly with entrectinib, making it a much weaker binder with both mutants than the wild-type. The alignments of amino acid sequences show that *NTRK1* mutations p.G595 (**D**) and p.G667 (**E**) are conserved among 6 clinically relevant tyrosine kinases listed in the figure. Both alterations are located in a residue homologous to amino acid changes involved in acquired resistance to therapies targeting other tyrosine kinases.

three prior lines of therapy, including anti-EGFR inhibition (4). However, after 4 months of treatment, resistance developed in this patient. The entrectinib half-life is 17 to 44 hours, and the intermittent dosing regimen may have promoted or anticipated the development of resistance due to incomplete treatment coverage of the patient. Nevertheless, it is still unknown whether or not continuous dosing will affect the emergence and/or the type of acquired mutations.

In this work, we sought to identify mechanisms of resistance to entrectinib, as this is key to the development of additional lines of therapy for patients carrying *NTRK1* rearrangements. The most commonly used approach to study resistance to targeted therapies involves molecular profiling of tissue biopsy obtained at progression. However, tumor heterogeneity and tissue sampling limit the effectiveness of this strategy. In addition, tissue biopsies are not always feasible and are associated with nonnegligible risks (16). Most importantly, even when the biopsy reveals emergence of alleles that were not present before treatment, their functional role in driving resistance remains to be formally established using functional assays. This requires significant experimental efforts, and the timeframe is not compatible with further treatment of the patient from whom the biopsy was obtained. We find that coupling pharmacologic analyses of xenopatients with molecular profiles of liquid biopsies allows the identification of resistance mechanisms in parallel with clinical treatment of individual patients, thus potentially enabling decisions on subsequent treatment options.

We report for the first time that acquisition of p.G595R and p.G667C mutations in the kinase domain of TRKA drives secondary resistance to TRK inhibition in colorectal cancer cells carrying *NTRK1* rearrangements. Both mutations were detected in patient plasma obtained at progression, suggesting that both are indeed associated with acquired resistance

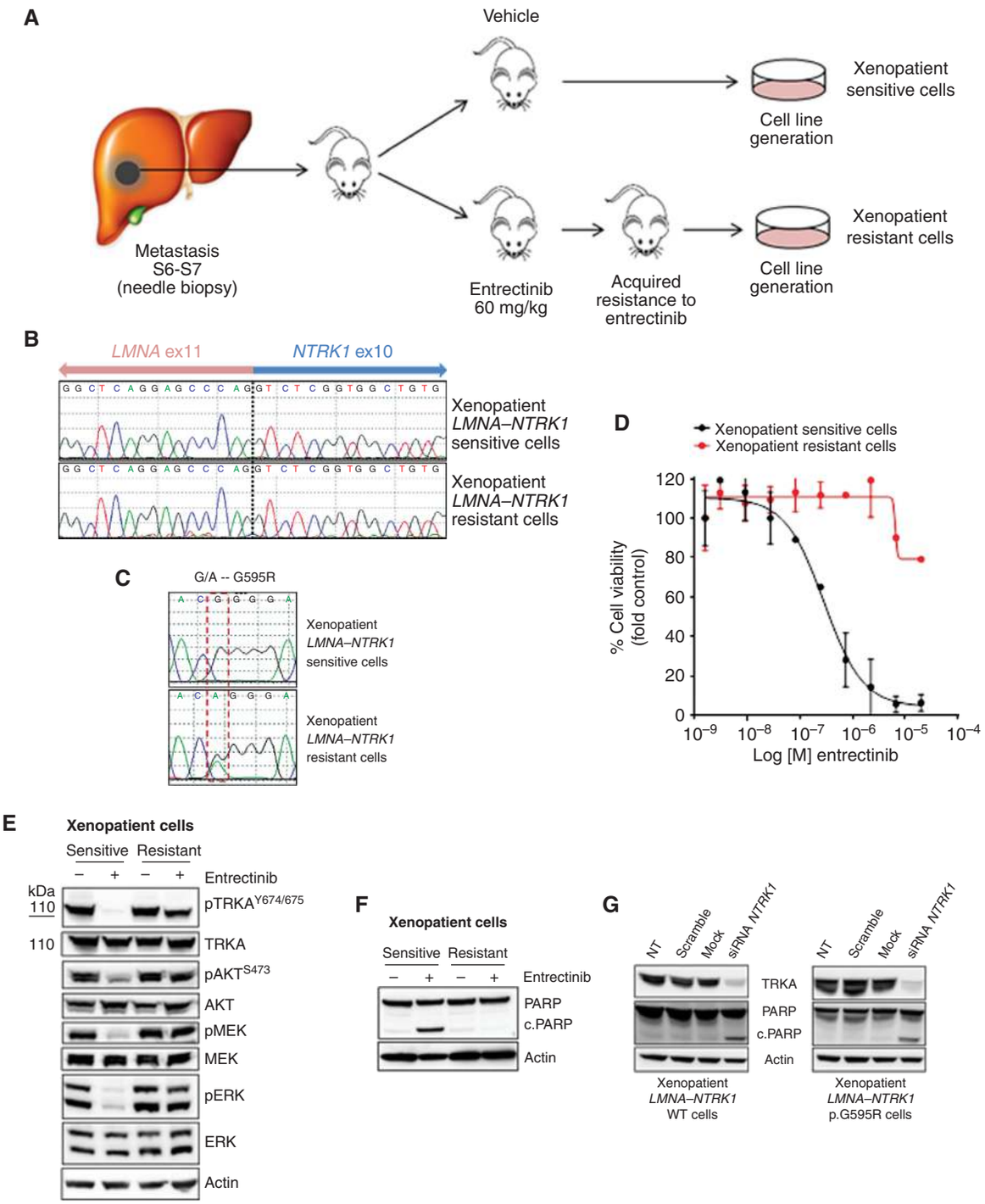

Figure 4. Biochemical and pharmacologic characterization of xenopatient-derived colorectal cancer cells. **A,** colorectal cancer cells were established from a vehicle-treated xenopatient (sensitive to entrectinib) and from the tumor grown in xenopatient #4 that became resistant to entrectinib treatment *in vivo*. **B,** Sanger sequencing electropherogram shows *LMNA–NTRK1* genetic rearrangements in both xenopatient-derived cell lines. **C,** cells derived from the xenopatient that developed resistance to entrectinib display *NTRK1* p.G595R mutation. **D,** drug proliferation assay of *LMNA–NTRK1*-rearranged colorectal cancer cells. Entrectinib-sensitive cells established from vehicle-treated xenopatient are indicated with black line; entrectinib-resistant cells established from resistant xenopatient are indicated with the red line. Cell viability was assessed by measuring ATP content after 5 days of treatment. **E,** sensitive and resistant xenopatient-derived cells were treated with 1 μmol/L entrectinib for 16 hours; after that, protein lysates were analyzed by Western blot. **F,** sensitive and resistant xenopatient-derived cells were treated with 1 μmol/L entrectinib for 48 hours; after that, protein lysates were analyzed by Western blot. **G,** RNAi knockdown of WT *NTRK1* in xenopatient-derived sensitive cells and mutated *NTRK1* in xenopatient-derived resistant cells induces apoptosis, as shown by cleaved PARP (c.PARP). Protein lysates were analyzed by Western blot 3 days after transfection with *NTRK1*-specific pooled siRNAs, scrambled siRNA, or transfection reagent (mock).

to entrectinib in the clinical setting. We found a remarkable concordance among results obtained in clinical samples and preclinical models. Genomic profiling of patient-derived samples and multiple cell models pointed to the p.G595R or p.G667C *NTRK1* mutations as the only common mechanism of resistance to entrectinib.

Analysis of a larger number of patients will ultimately be needed to determine the clinical impact of the findings. Based on data obtained with other kinase inhibitors, it is possible that other mechanisms of resistance to entrectinib could occur, including activation of parallel pathways able to bypass TRKA inhibition.

Interestingly, we found that the emergence of each of the two mutations might be dependent on the entrectinib concentration used. *NTRK1* p.G667C emerged when cells were exposed to a low concentration of the inhibitor, whereas it was absent from cells made resistant to higher dose.

Structural model–based characterization also indicates that the potency of the p.G667C mutation in conferring resistance to entrectinb is weaker than p.G595R. Both mutations fall in the ATP binding pocket and are analogous to resistance mutations that have been described for other clinically druggable tyrosine kinase fusions. Although p.G595C completely abrogates the binding of entrectinib to TRKA, the p.G667C only reduces affinity of binding. In line with this, homology alignment showed that TRKA p.G595R is analogous to ALK p.G1202R, whereas TRKA p.G667C is analogous to ALK p.G1269A. Accordingly, ALK p.G1269A, which mediates resistance to crizotinib, can be overcome with second-generation ALK inhibitors, such as ceritinib and alectinib, whereas both are ineffective on ALK p.G1202R (17–19). Analogously, at clinically achievable doses, entrectinib still retains a partial effect on p.G667C but not on p.G595R TRKA.

Of note, although we found that cells that develop entrectinib resistance remain dependent on the expression of TRKA, none of the TRK inhibitors currently being tested in the clinic (LOXO-101 and TSR-011) can overcome resistance driven by p.G595R. Accordingly, the biochemical and pharmacologic characterization of the preclinical models described here highlights the need for developing next-generation TRKA inhibitors that do not rely on specific spatial accommodation of the drug–target interaction around the G595 region, aimed at overcoming resistance driven by the p.G595R variant.

In addition to providing clues for the development of second-generation TRK inhibitors, our finding offers a means of tracking—noninvasively—the emergence of resistance to entrectinib. Monitoring of *NTRK1* resistant variants (p.G595R and p.G667C) in the plasma of patients treated with entrectinib could be valuable to predict recurrences.

METHODS

Cell Line Authentication

KM12 colorectal cancer cells were obtained from the NCI60 cell line bank and authenticated in May 2011. The genetic identity of the cell line was last checked not fewer than 3 months before performing experiments by the Cell ID System and by Gene Print 10 System (Promega), through short tandem repeats (STR) at 10 different loci (D5S818, D13S317, D7S820, D16S539, D21S11, vWA, TH01, TPOX, CSF1PO, and amelogenin). Amplicons from multiplex PCRs were separated by capillary electrophoresis (3730 DNA Analyzer; Applied Biosystems) and analyzed using GeneMapperID software from Life Technologies. Cell lines were tested and resulted negative for *Mycoplasma* contamination with the Venor GeM Classic Kit (Minerva Biolabs).

Establishment of Primary Colorectal Cancer Cell Lines

Primary colorectal cancer cell lines were established from tumor tissues obtained from patient-derived xenografts. Tumor tissues were dissociated into single-cell suspension by mechanical dissociation using the gentleMACS Dissociator (Miltenyi Biotec) and enzymatic degradation of the extracellular matrix using the Tumor Dissociation Kit (Miltenyi Biotec) according to the manufacturer's instructions. The cell suspension was then centrifuged at 1,200 rpm for 5 minutes. Supernatants were removed and cell pellets were resuspended with DMEM/F12 medium containing 10% FBS. This process was repeated three times. Then, cell suspensions were filtered through a 70-μm cell strainer (Falcon) and resuspended with culture medium DMEM-F12 containing 2 mmol/L l-glutamine, antibiotics (100 U/mL penicillin and 100 μg/mL streptomycin), gentamicin 50 μg/mL, and 10 μmol/L ROCK inhibitor Y-27632 (Selleck Chemicals Inc.).

Ba/F3–TPM3–TRKA WT, G595R, and G667C Generation

To generate Ba/F3 cells expressing TPM3–TRKA WT, TPM3–TRKA G595R, and TPM3–TRKA G667C, the cDNAs were cloned from KM12 cells by RT-PCR and inserted into a lentiviral vector pVL-EF1a-MCS-IRES-Puro (BioSettia). After confirmation by direct sequencing, VSVG-pseudo-typed lentiviruses were introduced into murine IL3-dependent pro-B cell line Ba/F3. The transduced Ba/F3 cells were selected at 1 μg/mL of puromycin in the murine IL3-containing RPMI and 10% FBS media for 2 weeks. The stable cell pools were further selected in RPMI and 10% FBS media without murine IL3 for 4 weeks.

Drugs

Entrectinib, LOXO-101 (20), and TSR-011 (21) were obtained from Ignyta.

Patient's Sample Collection

Patient's plasma and tumor biopsy were obtained through protocols approved by the local Ethical Committee at Ospedale Niguarda Ca' Granda, Milan, Italy. The study was conducted according to the provisions of the Declaration of Helsinki, and the patient signed and provided informed consent before sample collection. The liver biopsy was subcutaneously implanted in NOD-SCID mouse according to a study protocol approved by the Ethical Committee at Ospedale Niguarda Ca' Granda, Milan, Italy, and the animal procedures approved by the Ethical Commission of the Institute for Cancer Research and Treatment and by the Italian Ministry of Health.

ddPCR Analysis

Isolated circulating free DNA was amplified using ddPCR Supermix for Probes (Bio-Rad) with the *LMNA–NTRK1* translocation, *NTRK1* p.G595R and *NTRK1* p.G667C assays (sequences of custom-designed probes are listed in Supplementary Table S5). ddPCR was then performed according to the manufacturer's protocol, and the results are reported as a percentage or fractional abundance of mutant DNA alleles to total (mutant plus wild-type) DNA alleles. DNA template (8–10 μL) was added to 10 μL of ddPCR Supermix for Probes (Bio-Rad) and 2 μL of the primer and probe mixture. This reaction mix was added to a DG8 cartridge, together with 60 μL of Droplet Generation Oil for Probes (Bio-Rad) and used for droplet generation. Droplets were then transferred to a 96-well plate (Eppendorf) and then thermal cycled with the following conditions:

5 minutes at 95°C, 40 cycles of 94°C for 30 seconds, 55°C for 1 minute followed by 98°C for 10 minutes (Ramp Rate 2°C/s). Droplets were analyzed with the QX200 Droplet Reader (Bio-Rad) for fluorescent measurement of FAM and HEX probes. Gating was performed based on positive and negative controls, and mutant populations were identified. The ddPCR data were analyzed with QuantaSoft analysis software (Bio-Rad) to obtain fractional abundance of the mutated alleles in the wild-type or normal background. The quantification of the target molecule was presented as a number of total copies (mutant plus WT) per sample in each reaction. The number of positive and negative droplets is used to calculate the concentration of the target and reference DNA sequences and their Poisson-based 95% confidence intervals, as previously shown (22). ddPCR analysis of normal control plasma DNA (from cell lines) and no DNA template controls were always included. Samples with too-low positive events were repeated at least twice in independent experiments to validate the obtained results.

NGS Analysis

Libraries were prepared with the Nextera Rapid Capture Custom Enrichment Kit (Illumina, Inc.), according to the manufacturer's protocol. Preparation of libraries was performed using up to 150 ng of plasma ctDNA and 100 ng of gDNA from both cells and avatar fresh tissue. gDNA was fragmented using transposons, adding simultaneously adapter sequences. For ctDNA libraries preparation, we used the NEBNext Ultra DNA Library Prep Kit for Illumina (New England BioLabs Inc.) with optimized protocol. Purified gDNA was isolated after the fragmentation step, and ctDNA were used as a template for subsequent PCR to introduce unique sample barcodes. Fragments' size distribution of the DNA was assessed using the 2100 Bioanalyzer with a High Sensitivity DNA assay kit (Agilent Technologies). An equal number of DNA libraries were pooled and subjected to targeted panel hybridization capture. Libraries were then sequenced using the Illumina MiSeq sequencer (Illumina, Inc.).

Bioinformatic Analysis

FastQ files generated by Illumina sequencer were mapped to the human reference (assembly hg19) using the BWA-mem algorithm (23); PCR duplicates were then removed using the SAMtools package (24). Xenome software (25) was applied to remove murine sequences from xenopatient samples prior to alignment. We used a custom pipeline for NGS (10) in order to call somatic variations when supported by at least 1.5% allelic frequency and 5% significance level obtained with a Fisher test. Mutational analyses were the result of comparison between pretreatment and posttreatment samples.

Detection of LMNA–NTRK1 *Rearrangement in ctDNA*

ctDNA obtained from blood draw collected before entrectinib treatment started was analyzed by NGS as described above. To unveil the specific *LMNA–NTRK1* genetic rearrangement, a combination of BWA (v. 0.7.10) and BLAT (v. 35) was used. BWA was first used to align reads to the hg19 human reference genome with default options. The reads with a nonperfect alignment from BWA, potentially containing translocations, were extracted and aligned using BLAT (tileSize 11 and stepSize 5). The resulting PSL alignment was then post-processed to detect chimeric alignments. Gene fusion calling was performed using the following criteria: (i) each fusion partner must have at least 25 mapped bases on the respective end of the read; (ii) the fusion partners must map to two different genes; (iii) each reported fusion breakpoint must be supported by at least 10 reads. Based on the fusion sequence identified by NGS analysis, specific ddPCR primers and probes for the *LMNA–NTRK1* rearrangement were designed using Primer3 Input (version 0.4.0) following BioRad instructions available on the website. Primers and probe sequences are listed in Supplementary Table S5.

Kinase Domain Alignment

The amino-acidic sequences of human TRKA [P04629], ALK [Q9UM73], ROS1 [P08922], EGFR [P00533], KIT [P10721], and MET [P08581] were obtained from the UniprotKB database (26). Their kinase domains were aligned using the MUSCLE tool (27) and results were post-processed using Jalview (28).

Disclosure of Potential Conflicts of Interest

R. Wild has ownership interest (including patents) in Ignyta, Inc. A. Bardelli is a consultant/advisory board member for Horizon Discovery, Trovagene, and Biocartis. No potential conflicts of interest were disclosed by the other authors.

Authors' Contributions

Conception and design: M. Russo, S. Misale, G. Wei, R. Wild, G. Li, S. Siena, A. Bardelli

Development of methodology: S. Misale, G. Wei, G. Siravegna, B. Mussolin, R. Wild, S. Siena

Acquisition of data (provided animals, acquired and managed patients, provided facilities, etc.): M. Russo, S. Misale, G. Wei, G. Siravegna, L. Lazzari, B. Mussolin, A. Bartolini, N. Cam, R. Patel, A. Sartore-Bianchi, S. Siena

Analysis and interpretation of data (e.g., statistical analysis, biostatistics, computational analysis): M. Russo, S. Misale, G. Wei, G. Siravegna, G. Crisafulli, G. Corti, G. Rospo, L. Novara, B. Mussolin, N. Cam, R. Patel, S. Yan, R. Shoemaker, R. Wild, G. Li, S. Siena, A. Bardelli

Writing, review, and/or revision of the manuscript: M. Russo, S. Misale, G. Wei, G. Siravegna, G. Crisafulli, G. Corti, L. Novara, A. Bartolini, S. Yan, R. Wild, F. Di Nicolantonio, A. Sartore-Bianchi, G. Li, S. Siena, A. Bardelli

Administrative, technical, or material support (i.e., reporting or organizing data, constructing databases): B. Mussolin, N. Cam, G. Li, S. Siena

Study supervision: G. Wei, G. Li, S. Siena, A. Bardelli

Grant Support

This study was financially supported by the European Community's Seventh Framework Programme under grant agreement no. 602901, MErCuRIC (A. Bardelli); Innovative Medicines Initiative grant no. 115749, CANCER-ID (A. Bardelli); Associazione Italiana per la Ricerca sul Cancro (AIRC) IG grant no. 12812 (A. Bardelli); AIRC 2010 Special Program Molecular Clinical Oncology 5 per mille, project no. 9970 (A. Bardelli); FPRC 5 per mille 2010 and 2011 Ministero della Salute (F. Di Nicolantonio and A. Bardelli); and Ministero dell'Istruzione, dell'Università e della Ricerca, progetto PRIN (A. Bardelli). Investigators at Niguarda Cancer Center (A. Sartore-Bianchi and S. Siena) are also supported by Fondazione Oncologia Niguarda Onlus.

The costs of publication of this article were defrayed in part by the payment of page charges. This article must therefore be hereby marked *advertisement* in accordance with 18 U.S.C. Section 1734 solely to indicate this fact.

Received August 3, 2015; revised October 31, 2015; accepted November 4, 2015; published OnlineFirst November 6, 2015.

REFERENCES

1. Vaishnavi A, Le AT, Doebele RC. TRKing down an old oncogene in a new era of targeted therapy. Cancer Discov 2015;5:25–34.
2. Shaw AT, Hsu PP, Awad MM, Engelman JA. Tyrosine kinase gene rearrangements in epithelial malignancies. Nat Rev Cancer 2013;13:772–87.

3. Siena S, Drilon AE, Ou S-HI, Farago AF, Patel M, Bauer TM, et al. Entrectinib (RXDX-101), an oral pan-Trk, ROS1, and ALK inhibitor in patients with advanced solid tumors harboring gene rearrangements. Eur J Cancer 2015;50:Supplement 3.
4. Sartore-Bianchi A, Ardini E, Bosotti R, Amatu A, Valtorta E, Somaschini A, et al. Sensitivity to entrectinib associated with a novel LMNA–NTRK1 gene fusion in metastatic colorectal cancer. J Natl Cancer Int 2016;108. [Epub ahead of print].
5. Ardini E, Bosotti R, Borgia AL, De Ponti C, Somaschini A, Cammarota R, et al. The TPM3–NTRK1 rearrangement is a recurring event in colorectal carcinoma and is associated with tumor sensitivity to TRKA kinase inhibition. Mol Oncol 2014;8:1495–507.
6. Vaishnavi A, Capelletti M, Le AT, Kako S, Butaney M, Ercan D, et al. Oncogenic and drug-sensitive NTRK1 rearrangements in lung cancer. Nat Med 2013;19:1469–72.
7. Medico E, Russo M, Picco G, Cancelliere C, Valtorta E, Corti G, et al. The molecular landscape of colorectal cancer cell lines unveils clinically actionable kinase targets. Nat Commun 2015;6:7002.
8. Siravegna G, Bardelli A. Genotyping cell-free tumor DNA in the blood to detect residual disease and drug resistance. Genome Biol 2014;15:449.
9. Misale S, Yaeger R, Hobor S, Scala E, Janakiraman M, Liska D, et al. Emergence of KRAS mutations and acquired resistance to anti-EGFR therapy in colorectal cancer. Nature 2012;486:532–6.
10. Siravegna G, Mussolin B, Buscarino M, Corti G, Cassingena A, Crisafulli G, et al. Clonal evolution and resistance to EGFR blockade in the blood of colorectal cancer patients. Nat Med 2015;21:795–801.
11. Hindson BJ, Ness KD, Masquelier DA, Belgrader P, Heredia NJ, Makarewicz AJ, et al. High-throughput droplet digital PCR system for absolute quantitation of DNA copy number. Anal Chem 2011;83:8604–10.
12. Reinert T, Schøler LV, Thomsen R, Tobiasen H, Vang S, Nordentoft I, et al. Analysis of circulating tumour DNA to monitor disease burden following colorectal cancer surgery. Gut 2015. [Epub ahead of print].
13. Stransky N, Cerami E, Schalm S, Kim JL, Lengauer C. The landscape of kinase fusions in cancer. Nat Commun 2014;5:4846.
14. Wiesner T, He J, Yelensky R, Esteve-Puig R, Botton T, Yeh I, et al. Kinase fusions are frequent in Spitz tumours and spitzoid melanomas. Nat Commun 2014;5:3116.
15. Bounacer A, Schlumberger M, Wicker R, Du-Villard JA, Caillou B, Sarasin A, et al. Search for NTRK1 proto-oncogene rearrangements in human thyroid tumours originated after therapeutic radiation. Br J Cancer 2000;82:308–14.
16. Overman MJ, Modak J, Kopetz S, Murthy R, Yao JC, Hicks ME, et al. Use of research biopsies in clinical trials: are risks and benefits adequately discussed? J Clin Oncol 2013;31:17–22.
17. Friboulet L, Li N, Katayama R, Lee CC, Gainor JF, Crystal AS, et al. The ALK inhibitor ceritinib overcomes crizotinib resistance in non–small cell lung cancer. Cancer Discov 2014;4:662–73.
18. Katayama R, Friboulet L, Koike S, Lockerman EL, Khan TM, Gainor JF, et al. Two novel ALK mutations mediate acquired resistance to the next-generation ALK inhibitor alectinib. Clin Cancer Res 2014;20:5686–96.
19. Zou HY, Friboulet L, Kodack DP, Engstrom LD, Li Q, West M, et al. PF-06463922, an ALK/ROS1 inhibitor, overcomes resistance to first and second generation ALK inhibitors in preclinical models. Cancer Cell 2015;28:70–81.
20. Doebele RC, Davis LE, Vaishnavi A, Le AT, Estrada-Bernal A, Keysar S, et al. An oncogenic NTRK fusion in a patient with soft-tissue sarcoma with response to the tropomyosin-related kinase inhibitor LOXO-101. Cancer Discov 2015;5:1049–57.
21. Wilcoxen KM, inventor; Tesaro, Inc., assignee. Modulating certain tyrosine kinases. United States patent US wo2013074518a1 2013 May 23.
22. Hayden RT, Gu Z, Ingersoll J, Abdul-Ali D, Shi L, Pounds S, et al. Comparison of droplet digital PCR to real-time PCR for quantitative detection of cytomegalovirus. J Clin Microbiol 2013;51:540–6.
23. Li H, Durbin R. Fast and accurate long-read alignment with Burrows-Wheeler transform. Bioinformatics 2010;26:589–95.
24. Li H, Handsaker B, Wysoker A, Fennell T, Ruan J, Homer N, et al. The Sequence Alignment/Map format and SAMtools. Bioinformatics 2009;25:2078–9.
25. Conway T, Wazny J, Bromage A, Tymms M, Sooraj D, Williams ED, et al. Xenome—a tool for classifying reads from xenograft samples. Bioinformatics 2012;28:i172–8.
26. Wu CH, Apweiler R, Bairoch A, Natale DA, Barker WC, Boeckmann B, et al. The Universal Protein Resource (UniProt): an expanding universe of protein information. Nucleic Acids Res 2006;34(Database issue):D187–91.
27. Edgar RC. MUSCLE: a multiple sequence alignment method with reduced time and space complexity. BMC Bioinformatics 2004;5:113.
28. Waterhouse AM, Procter JB, Martin DM, Clamp M, Barton GJ. Jalview Version 2–a multiple sequence alignment editor and analysis workbench. Bioinformatics 2009;25:1189–91.